Benthic ostracod diversity and biogeography in an urban semi–enclosed eutrophic riverine bay

Jialu Huang[1,2,3], Moriaki Yasuhara[2,3], He Wang[2,3,4], Pedro Julião Jimenez[2,3], Jiying Li[3,5], Minhan Dai[1]

[1]State Key Laboratory of Marine Environmental Science, College of Ocean and Earth Sciences, Xiamen University, Zhou
5 Long Quan Building, 4221 Xiang'an South Road, Xiamen 361102, China
[2]School of Biological Sciences, Area of Ecology and Biodiversity, Swire Institute of Marine Science, Institute for Climate
and Carbon Neutrality and Musketeers Foundation Institute of Data Science, The University of Hong Kong, Kadoorie
Biological Sciences Building, Pokfulam Road, Hong Kong SAR, China
[3]State Key Laboratory of Marine Pollution, City University of Hong Kong, Tat Chee Avenue, Kowloon, Hong Kong SAR,
10 China
[4]Nanjing Institute of Geology and Palaeontology, Chinese Academy of Sciences, 39 East Beijing Road, Nanjing 210008,
China
[5]Department of Ocean Science, Center for Ocean Research in Hong Kong and Macau, The Hong Kong University of Science
and Technology, Clear Water Bay, Kowloon, Hong Kong SAR, China

15 *Correspondence to*: Jialu Huang (jialuhuang@stu.xmu.edu.cn), Moriaki Yasuhara (yasuhara@hku.hk;
moriakiyasuhara@gmail.com), and He Wang (hwang@nigpas.ac.cn; wanghe0701@163.com)

Abstract. The benthic ecosystem has been greatly altered by environmental pressure over the past several decades.
Compared to some well-studied large bays, the situation will be in populated small bay areas is still under investigated. In
this study, we investigated the abundance, diversity, composition, and distribution of ostracod (a meiobenthic group) and
20 their interactions with eutrophication and pollution through high resolution sampling of surface sediment in Deep Bay, a
small semi-enclosed riverine bay adjacent to two of the world's most populated cities. We found that ostracod abundance
and diversity exhibited an inner-outer gradient in Deep Bay, shaped by eutrophication and pollution from human activities.
Faunal composition was also characterized by inner-outer difference, as well as difference between Hong Kong side and
Shenzhen side, where Hong Kong side was more influenced by eutrophication, Shenzhen side was more affected by metal
25 pollution. Ostracod distribution and their environmental preference in Deep Bay were consistent with broader studies in
Hong Kong, strongly supporting the idea that ostracod is a useful bioindicator of coastal benthic ecosystems. Our study
emphasizes the importance of studying of uncomplicated system with finer sampling, as this approach offers a clear and
direct understanding of how benthic ecosystems are shaped by distinct coastal environmental problems.

30 **1 Introduction**

Coastal bays that are highly influenced by adjacent populated cities are facing incremental environmental problems and
ecosystem degradation due to poor water exchange and intensive human activities (Dai et al., 2023; Nichols et al., 2019;
Breitburg et al., 2018). River discharge, aquaculture, maritime activities cause eutrophication and pollution of coastal areas,

ultimately leading altered marine biological diversity (Glibert, 2017). Deep Bay is a semi-closed bay influenced by several small rivers inside the bay and connected with Pearl River Estuary outside the bay. The bay is surrounded by Hong Kong and Shenzhen, two of the world's largest urbanized cities with 17.8 and 7.5 million people, respectively. It is also a well-known region for both oyster culture and hinterland mangrove ecosystem (Mohyuddin et al., 2023; Feng et al., 2020). Under the influence of nutrient and pollution inputs from rivers, the aquaculture industry, and large-scale reclamation projects, combined with limited water exchange, Deep Bay is currently experiencing increasing environmental degradation (Xu et al., 2019).

Benthic ecosystem alteration has been recognized as a main consequence of environmental degradation (Dorgham, 2014). Ostracoda (Crustacea), which is abundantly fossilized in marginal-marine sediments, has been used as a useful metazoan group bioindicator (Yasuhara et al., 2007). Previous studies in Hong Kong coast have suggested that ostracods can be used as a bioindicator for the diversity and biogeography of broader soft sediment benthos (Hong et al., 2022; Mamo et al., 2023). Statistical relationships between ostracod and environmental factors have been indicated (Hong et al, 2019). On this topic, some large, populated bays including Chesapeake Bay (Cronin and Vann, 2003), Osaka Bay (Yasuhara et al., 2007) and Baltic Sea (Frenzel et al., 2010) were well studied; small bays with less population were also investigated before (e.g., Irizuki et al., 2015). However, semi-enclosed, intensively human-influenced small bay areas remain under-studied, especially with high resolution sampling.

Previous studies in Deep Bay have primarily focused on sediment chemistry (Lee, 2000), pollutants (Zhang et al., 2021; Li et al., 2024), land reclamation (Ren et al., 2011) and mangrove restoration (Feng et al., 2020). Some ecological studies were conducted sorely in mangrove reserves (Zan et al., 2003). And due to the boundary control of the sea area, sampling has typically been restricted to on side (either Hong Kong side or Shenzhen side only). As a result, detailed biodiversity and biogeographic distributions for marine organisms in the broader area of Deep Bay are largely unknown.

In our study, we provided a comprehensive understanding on benthic community distribution and related environmental factors in Deep Bay, a small semi-enclosed bay adjacent to two of the world's largest cities. We investigated the geographical structure of ostracod abundance, diversity and composition, and how they interacted with eutrophication and pollution through doing high resolution sampling of surface sediments on both Hong Kong and Shenzhen sides of the bay.

2 Materials and methods

2.1 Site description

65 Deep Bay (22.41–22.53° N, 113.88–114.00° E) is located between the Shenzhen Special Economic-Zone of China and Hong Kong Special Administrative Region in the eastern part of Pearl River Estuary (Fig. 1). At 17 km long and 4–10 km wide, it is a semi-enclosed bay with limited water exchange. The main rivers flowing into the bay include the Shenzhen River and Shan Pui River in Hong Kong (Fig. 1). The hydrography of the bay is also strongly influenced by the discharge from the Pearl River. Deep Bay features a semidiurnal tidal system, with an annual tidal range of 1.4 m (Feng et al., 2020). At the

70 north-eastern end of the bay are the Futian and Mai Po mangrove reserves (Fig. 1). Along the Hong Kong coast and in the central part of the bay, oyster farming rafts have expanded over last several decades (Bowler et al., 1984, Fig. 1). Deep Bay is experiencing rapid urbanization and population growth, accompanied by intensive human activities such as agricultural, municipal and industrial water discharge into the bay (Yang et al., 2021).

75
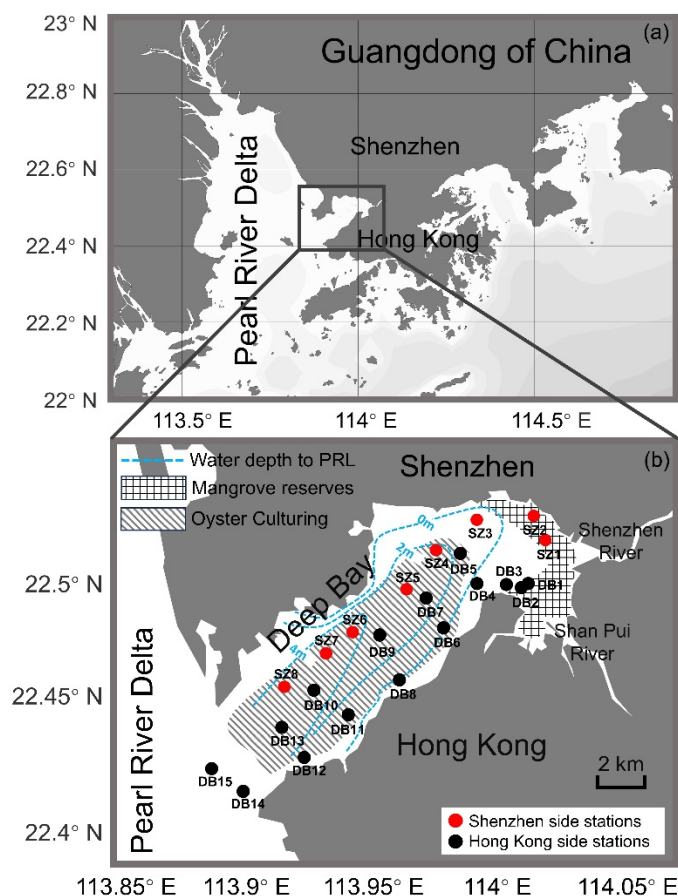
Figure 1. Locality map of Deep Bay and sampling sites. Red dots represent stations in the Shenzhen side sampled in July 2024. Black dots represent stations in the Hong Kong side sampled in September 2023. Grid filling represents Futian (north) and Mai Po (south) mangrove reserves (adapted from Feng et al., 2020). Dashed filling represents areas of oyster culturing in Deep Bay (adapted from Google Map). Blue dashed lines represent relative water depth to Pearl River Level (PRL) which reflect local
80 **bathymetry (adapted from Ye et al., 2018).**

2.2 Materials

2.2.1 Ostracod samples and processing

Surface sediment samples of 100 mL were collected by using a Ekman Grab from twenty three locations that cover entire

85 Deep Bay area (Fig. 1). Including fifteen sites collected in September, 2023 from the Hong Kong side, eight sites collected in

July, 2024 from the Shenzhen side. Several sites, including DB3, DB5, DB9, DB10, DB15, overlapped with the Hong Kong

Environmental Protection Department (EPD) monitoring stations DM1 (DS1), DM2, DM3 (DS2), DM4 (DS3), DM5 (DS4)

respectively (DM represents seawater quality monitoring stations and DS represents sediment quality monitoring stations; Environmental Protection Department, 2024).

90

Sediment samples were washed through a 63 μm sieve and dried at 40 °C in an oven. The dried samples were then sieved using a 150 μm sieve, and ostracod specimens larger than 150 μm were picked out for analysis. All individuals were picked out from the samples if the total number of specimens was less than 200. For samples containing substantially more than 200 specimens, we divided them into fractions using a sample splitter. The sample materials primarily consisted of death

95 assemblages, with some articulated carapaces and a few containing soft parts inside. Each single valve was considered one individual, each carapace was considered two individuals (Yasuhara et al., 2017).

2.2.2 Environmental variables and data compilation

Additional surface sediment samples were collected in the same stations from the same cruise above to examine total organic

100 carbon (TOC), total carbon (TC), total nitrogen (TN), total sulfur (TS) and their isotopes. Sediment chemical oxygen demand and the concentrations of heavy metals, including copper, chromium, barium, cadmium, mercury, and a pollutant total cyanide were obtained from EPD sediment monitoring stations DS1–4 (Environmental Protection Department, 2024). Data on bottom water hypoxia frequency (with threshold of 2 mg/L, 3 mg/L and 4 mg/L respectively), surface nutrient levels of dissolved inorganic nitrogen (DIN) and dissolved inorganic phosphorus (DIP), and physical parameters including bottom

105 temperature and salinity were obtained from EPD seawater monitoring stations DM1–5 (Environmental Protection Department, 2024). As our grab sampler penetrated about 10 cm into the sediments, and the sedimentation rate was approximately 1cm/yr in Deep Bay (Yan et al., 2019), we used recent ten years' average (2012–2022) of the sediment/seawater monitoring result for analysis. We also compiled perfluoroalkyl and polyfluoroalkyl substances (PFAs) and heavy metal data from recent studies (Zhang et al., 2021; Li et al., 2024), selecting sites in proximity to those in our

110 study.

2.3 Methods

2.3.1 Diversity analysis

We used Hill numbers, or the effective numbers of equally abundant species, to estimate ostracod diversity at each station or

115 group of stations. Hill number offers several major advantages and has been increasingly adopted by ecologists (Chao et al., 2020). The order q of Hill numbers represents the sensitivity of the diversity metric to species relative abundance. Specifically, Hill number ^{0}D with order q=0 measures species richness; ^{1}D measures the diversity of the abundant species,

and ^2D measures the diversity of dominant species (Chao et al., 2014). The Hill numbers ^1D and ^2D are equivalent to the exponential of Shannon entropy and Simpson diversity index, respectively (Chao et al., 2014).

120

2.3.2 Multivariate analysis

We applied hierarchical cluster analysis to measure the dissimilarity among ostracod fauna from different sites, using diversity decomposition to obtain dissimilarity measures. We also performed a non-metric Multidimensional Scaling (nMDS) to show faunal similarities among ostracod assemblages in two-dimensional space. We used dissimilarity indices of

125 Sørensen (Sørensen, 1948), Horn (Horn, 1966) and Morisita-Horn (Morisita, 1959), to estimate the effective proportion of unshared species in the ostracod assemblages. While classical Sørensen dissimilarity is presence-absence based, Horn and Morisita-Horn are designed to quantify the compositional dissimilarities of abundant and dominant species. The environmental variables we used for multivariate analysis included TOC, TC, TN, TS in sediment, heavy metals (As, Cd, Cu, Pb, Zn) adapted from Zhang et al (2021), PFAs adapted from Li et al (2024), ten years' average hypoxia frequency, pH, DIN

130 and Chlorophyll-a (*Chla*) calculated from EPD seawater monitoring data (Environmental Protection Department, 2024).

3 Results

3.1 Environmental settings

Deep Bay exhibited a riverine-oceanic salinity gradient from riverine freshwater input in the inner bay to more saline water

135 influenced by the Pearl River Estuary in the outer bay (Fig. 2c). This gradient is also reflected in other related parameters, such as nutrients (Fig. 2b), heavy metal and other pollutants (Fig. 2e, f), and TOC, TN levels (Fig. 3a, c). Hypoxia frequency was much higher in the inner bay than the outer bay, while surface DIN and DIP was higher in inner bay (Fig. 2a, b). Sediment chemical oxygen demand, heavy metal and other pollutants were relatively high in the inner bay and gradually decreased towards the outer bay (Fig. 2d–f). In the inner bay, besides the Shenzhen River and Shau Pui River, mangrove

140 forests expand along the coastline, forming the Futian and Mai Po mangrove reserves (Fig. 1). Oyster shelf expands throughout most of the remaining bay area, particularly in the central and Hong Kong side of the bay (Fig. 1). The bathymetry of the Deep Bay is high in the inner part and along the sides, while it is lower in the outer part of the bay (Ye et al., 2018, Fig. 1).

145 Eutrophication and pollution were predominant in the inner bay (Figs. 2, 3). Hypoxia frequency and nutrient concentration were elevated at EPD water monitoring stations DM1 and DM2 (Fig. 2a, b). Chemical oxygen demand, heavy metal and other pollutants in sediment were also relatively high at EPD sediment monitoring stations DS1 and DS2 in the inner bay (Fig. 2d–f). Our TOC and TN results showed the same trend that inner bay stations had higher values compared to the outer

stations (Fig. 3a, c). DB3 had the highest TOC and TN values, substantially exceeding those of the other sites (Fig. 3a, c).

150 The lower δ^{13}C-TOC and δ^{15}N-TN values in the inner bay indicated a predominant organic matter source from terrestrial detritus, while the higher values in the outer bay suggest a predominant organic matter source of marine origin (Fig. 3a–d). The negative linear relationship between δ^{13}C-TOC and TOC/TN of the entire bay indicated a mixing between marine algae (with higher δ^{13}C-TOC and lower TOC/TN value) and C3 terrestrial plants like mangrove (with lower δ^{13}C-TOC and higher TOC/TN value) (Fig. 3e, f).

155
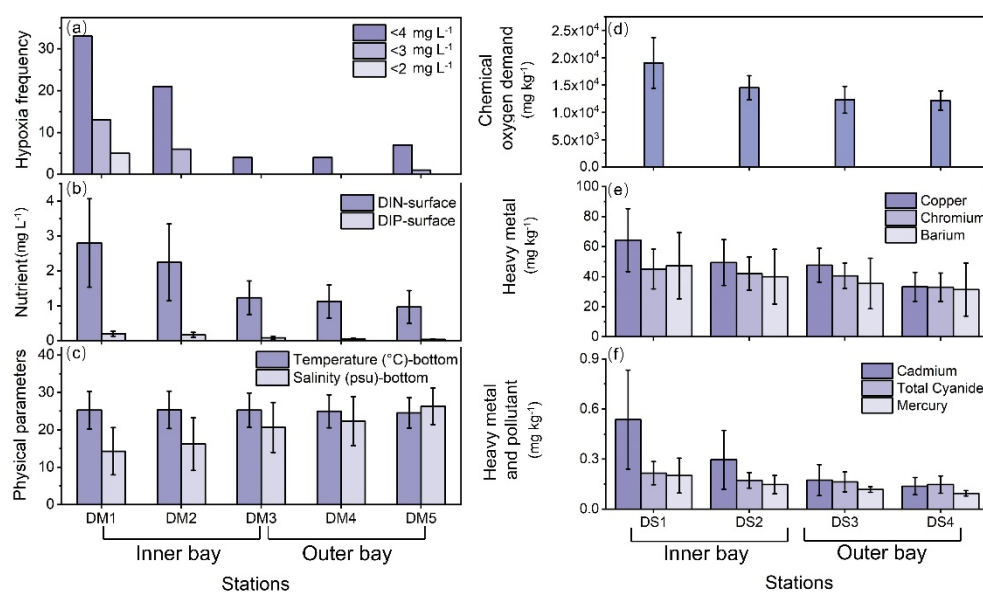
Figure 2. Sediment and seawater properties vary from inner bay to outer bay based on EPD monitoring data. Left panels (a–c) show bottom water hypoxia frequency (with threshold of 2mg/L, 3mg/L, 4mg/L respectively), surface nutrient DIN and DIP and physical parameters bottom temperature and salinity from DM1 to DM5. Right panels (d–f) show sediment chemical oxygen
160 **demand, and concentrations of heavy metal including copper, chromium, barium, cadmium, mercury and pollutant total cyanide from DS1 to DS4. The data are annual averages from 2012 to 2022.**
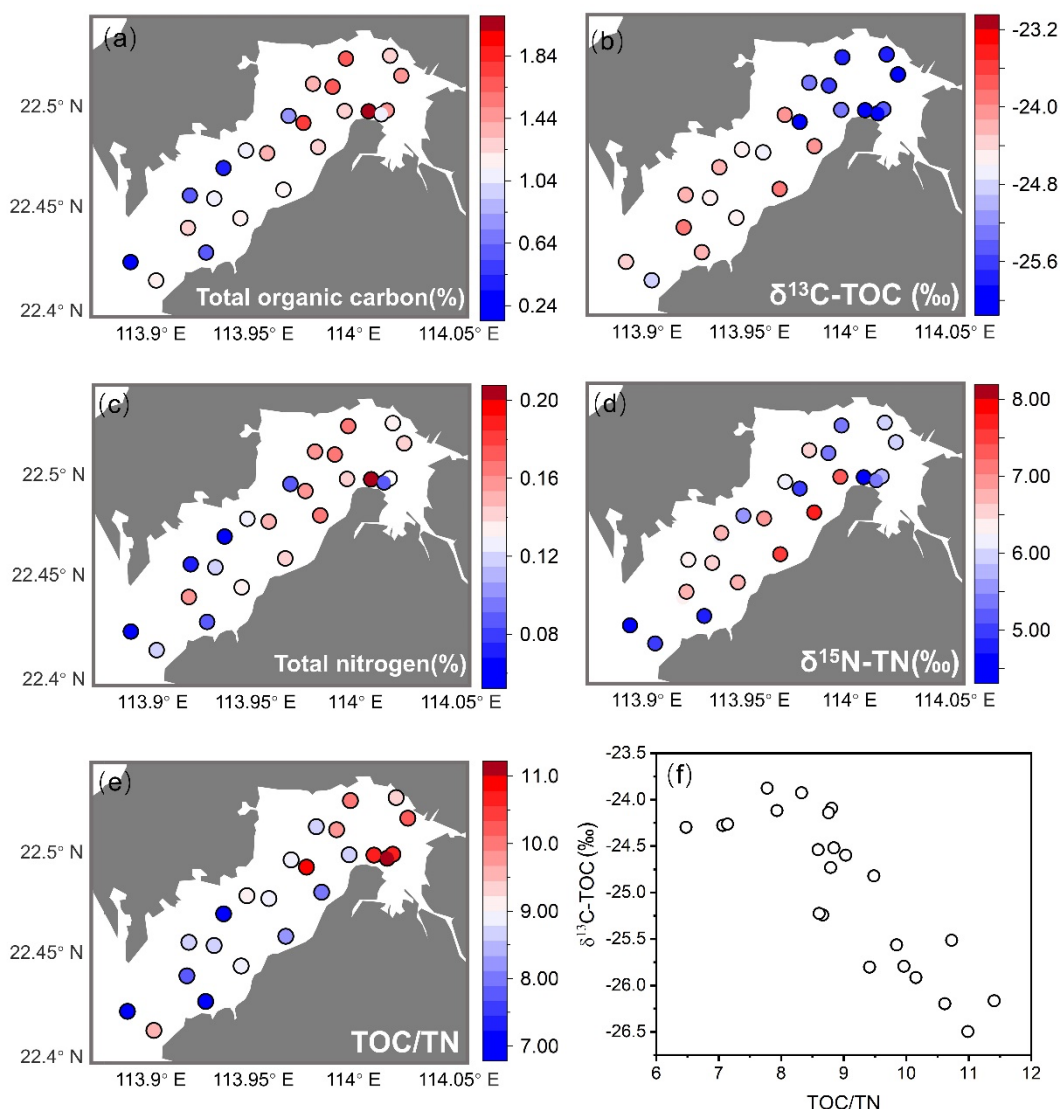
Figure 3. Elemental and their isotope analysis results in the sediments, including total organic carbon (%) (a) and its isotope (b), total nitrogen (%) (c) and its isotope (d), TOC/TN ratio (e), δ^{13}C-TOC and TOC/TN ratio relationship (f).

3.2 Abundance and diversity

Abundance of ostracods in Deep Bay generally followed a gradient corresponding to the environmental conditions from the inner to outer bay. There tend to be lower abundance in the inner bay sites, with abundance increasing exponentially toward the bay mouth (Fig. 4). The lowest abundance was found inside the mangrove conservation area with almost zero specimen

(Fig. 4). This may be due to the acidic conditions in mangrove sediments, which negatively affect the preservation of calcium carbonate ostracod shells (Plazziat et al., 1983). The inner bay, characterized by eutrophication and riverine conditions, generally had ostracod abundance below 100, while the outer bay exhibited much higher abundance, especially at sites DB12, DB14 and DB15 (Fig. 4).

175

The diversity of ostracods in Deep Bay similarly followed the same inner-outer bay gradient (Fig. 5). The number of species, indicated by Hill Number ^0D, was relatively high at the bay mouth sites SZ8, DB10, DB12, DB14 and DB15, ranging from 20 to 33. The other stations mostly had value below 10 (Fig. 5a). Similarly, the diversity of abundant species and dominant species (^1D and ^2D) were also higher among the stations at the bay mouth (Fig. 5b, c). Notably, DB7 and DB11 exhibited

180 relatively high diversity in both abundant and dominant species (Fig. 5b, c).
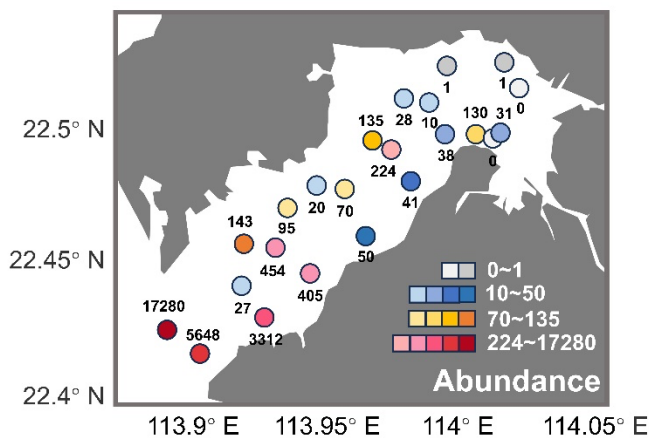
Figure 4. Ostracod abundance (total number of individuals per sample) in deep bay.
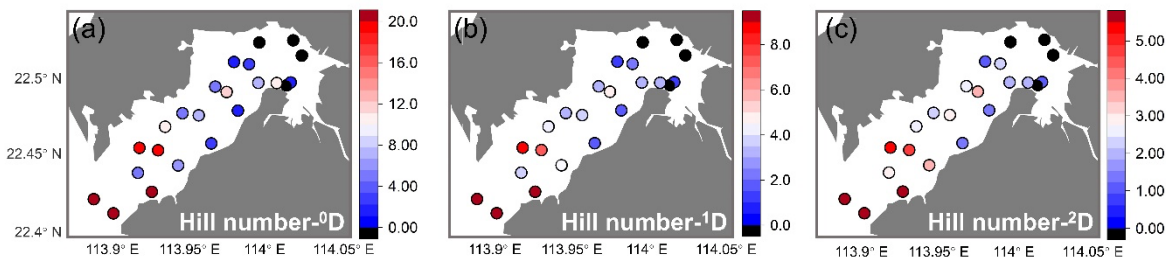
Figure 5. Diversity results of deep bay ostracods. Distribution of Hill numbers ^0D (q=0, species richness) (a), ^1D (q=1, exponential Shannon) (b) and ^2D (q=2, inversed Simpson) (c). Black dots represent stations with low abundance which are not included in the diversity calculation.

3.3 Multivariate analysis

Cluster analysis based on Sørensen, Horn and Morisita-Horn dissimilarities delineated biofacies considering faunal composition in terms of species occurrence, relative abundance of abundant species, and relative abundance of dominant species, respectively. These three dissimilarities all showed a relatively clear separation both in geographical distribution and nMDS results (Fig. 6). The nMDS results showed a separation of five biofacies based on Sørensen and Morisita-Horn and six biofacies based on Horn dissimilarity (Fig. 6a, c, e).

Sørensen dissimilarity showed a separation between inner bay and outer bay part of Deep Bay into biofacies 3 and biofacies 5, respectively (Fig. 6a). Inner bay part (biofacies 3) was related to almost all the environmental parameters we used (Fig. 6b), which showed that inner bay part was strongly influenced by eutrophication, hypoxia and pollutants. Biofacies 3 was characterized by the presence of *Cytherois* sp., *Loxoconcha sinensis*, *Paracypris* sp. and *Paracytherois* sp. as well as the absence of species that characterized other biofacies such as *Spinileberis bella* and *Spinileberis quadriaculeata* (Table 1). Biofacies 5 was characterized by the presence of marine species *Alocopocythere goujoni*, *Keijialla kloempritensis*, and *Xestoleberis hanaii* (Table 1). Except the two main groups above, inner bay biofacies 1 was characterized by the presence of *Spinileberis bella* and *Sinocytheridea impressa* and the absence of other species (Table 1). Biofacies 2 was characterized by the occurrence of brackish water species *Spinileberis bella*, *Spinileberis quadriaculeata*, *Loxoconcha ocellata*, and *Paracathaycythere* sp. (Table 1). Biofacies 4 was similar to biofacies 2 but distinguished by the occurrence of *Stigmatocythere bona* and *Propontocypris* sp. (Table 1).

Horn and Morisita-Horn dissimilarities revealed a distinction between Hong Kong side stations and Shenzhen side stations, i.e., the Hong Kong side group (biofacies 3) and the Shenzhen side group (biofacies 4) (Fig. 6c, e). The Hong Kong side group was more eutrophication-influenced and characterized by the dominance of *Sinocytheridea impressa* (Table 1), while the Shenzhen side group was more related to heavy metal and other polluants (Fig. 6d, f) and characterized by the dominance of *Neomonceratina delicata* (Table 1). Other biofacies were distributed in the bay mouth (biofacies 5) and inner bay (biofacies 1, 2, and 6) (Fig. 6c, e). The bay mouth biofacies 5 was unrelated to all eutrophication/pollution environmental parameters (Fig. 6), and characterized by moderately high aboundance of both *Sinocytheridea impressa* and *Neomonceratina delicata* without any distinctively dominant species (Table 1). The inner-most bay biofacies 1 was distinguished by the dominance of *Spinileberis bella* (Table 1). Biofacies 2 was distinguished by the dominance of *Bicornucythere bisanensis* s.l.

(Table 1). Biofacies 6 in Horn dissimilaity was less diverse and characterized by the dominance of *Neomonoceratina delicata* and *Neosinocythere elongata* (Table 1).
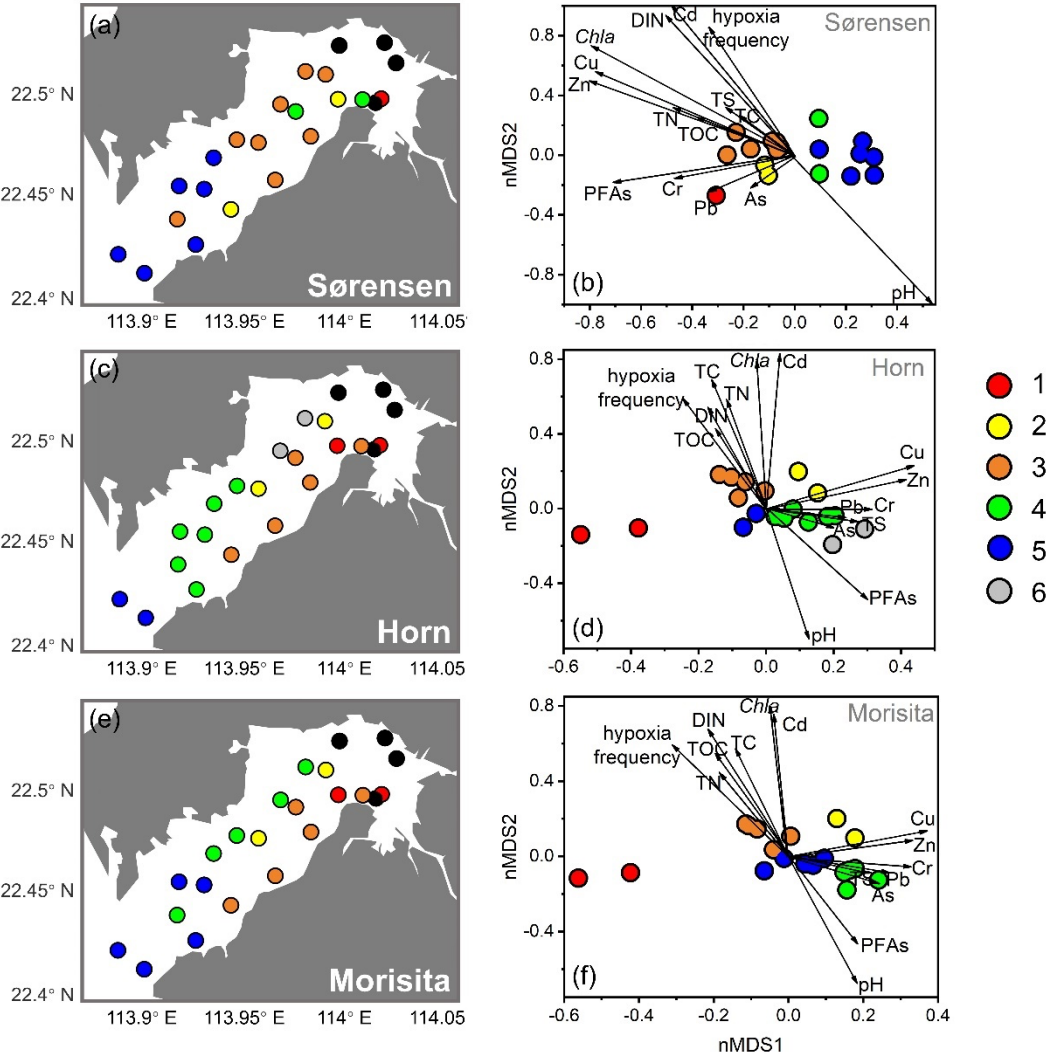
Figure 6. Distribution map in left panels (a, c, e) and nMDS ordination in right panels (b, d, f) showing biofacies based on Sørensen, Horn and Morisita-Horn dissimilarities. Vectors on the nMDS ordination show the strength and direction of relation between environmental variables and the nMDS axes. Black dots represent stations with low abundance which are not included in calculation.

Table 1. List of top 10 species with the highest (%) mean relative abundance for biofacies 1~6 based on Sørensen, Horn and Morisita-Horn dissimilarities. Specific biofacies among different dissimilarities may not be correspondingly related. Circular marks in the table represents corresponding biofacies showed in Fig. 6.

Dissimilarity	Species	1	2	3	4	5	6
Sørensen	*Alocopocythere goujoni*			3.10		5.27	
	Aurila sp.				0.83		
	Bicornucythere bisanensis s.l.		5.92	20.33	17.72	8.94	
	Cytherois sp.			1.85			
	Keijella kloempritensis					5.60	
	Loxoconcha sinensis			0.63			
	Loxoconcha ocellata		3.29				
	Neomonceratina delicata		17.76	40.93	14.64	34.53	
	Neosinocythere elongata		0.16	4.43	0.89	2.11	
	Paracathaycythere sp.		1.32				
	Paracypris sp.			0.54			
	Paracytherois sp.			0.18			
	Pistocythereis bradyformis				0.99	1.63	
	Pistocythereis bradyi		1.32			3.40	
	Propontocypris sp.				2.33		
	Sinocytheridea impressa	3.23	25.99	28.01	55.27	19.93	
	Spinileberis bella	96.77	41.61		0.89		
	Spinileberis quadriaculeata		2.63		1.12		
	Stigmatocythere bona				1.34	2.19	
	Xestoleberis hanaii					2.28	
Horn	*Alocopocythere goujoni*		0.71		7.82		2.96
	Aurila sp.					1.42	
	Bicornucythere bisanensis s.l.	1.32	54.29	9.73	12.51	6.71	7.65
	Cytherois sp.				3.59		
	Hemicytheridea reticulata				1.13		
	Keijella kloempritensis				0.99	13.84	
	Loxoconcha sinensis				1.24		
	Loxoconcha ocellata			1.32			
	Neomonceratina delicata	3.95	19.29	17.11	46.93	20.58	72.35
	Neosinocythere elongata		1.43	0.42		3.41	16.30
	Paracathaycythere sp.	1.32					

	Species						
	Paracypris sp.		2.14				
	Paracytherois sp.		0.71				
	Pistocythereis bradyformis			0.40		3.27	
	Pistocythereis bradyi	1.32				7.71	
	Propontocypris sp.			0.93		2.85	
	Sinocytheridea impressa	6.88	21.43	63.87	13.89	24.33	0.74
	Spinileberis bella	82.60		3.32			
	Spinileberis quadriaculeata	2.63		0.45			
	Stigmatocythere bona			0.54	1.55	1.92	
	Xestoleberis hanaii				1.80		
Morisita	*Alocopocythere goujoni*		0.71		6.56	4.43	
	Bicornucythere bisanensis s.l.	1.32	54.29	9.73	11.71	9.05	
	Cytherois sp.				3.17		
	Keijella kloempritensis				0.42	6.30	
	Loxoconcha sinensis				1.21		
	Loxoconcha ocellata			1.32			
	Neocyprideis agilis				0.21		
	Neomonceratina delicata	3.95	19.29	17.11	64.05	29.44	
	Neosinocythere elongata		1.43	0.42	6.94	2.11	
	Paracathaycythere sp.	1.32					
	Paracypris sp.		2.14				
	Paracytherois sp.		0.71				
	Pistocythereis bradyformis			0.40	0.42		
	Pistocythereis bradyi	1.32				4.07	
	Propontocypris sp.			0.93		1.71	
	Sinocytheridea impressa	6.88	21.43	63.87	5.09	21.60	
	Spinileberis bella	82.60		3.32			
	Spinileberis quadriaculeata	2.63		0.45			
	Stigmatocythere bona			0.54		2.42	
	Xestoleberis hanaii					2.73	

3.4 Biogeography

230 Geographical distribution of individual species were showed in Figs. 7 and 8. *Neomonoceratina delicata* was mostly distributed in the Shenzhen side (Fig. 7a). *Sinocytheridea impressa* had higher abundance in the Hong Kong side (Fig. 7b). *Spinileberis bella* was concentrated in the river mouth (Fig. 7c). *Bicornucythere bisanensis* s.l. was distributed with high abundance in the inner bay eutrophic/polluted area (Fig. 7d). *Alocopocythere goujoni* was distributed mostly in the outer bay, Shenzhen side (Fig. 7e). *Neosinocythere elongata* was abundant in an inner bay station SZ5 (Fig. 7f). *Keijiella*

235 *kloempritensis* was abundant only in the stations DB14 and DB15 located near the bay mouth (Fig. 7g). *Pistocythereis bradyi* was abundant in a bay mouth station DB15 (Fig. 7h). *Cytherois* sp. occurred mostly in an outer bay station DB13 (Fig. 7i). *Stigmatocythere bona* was abundant in outer bay stations SZ7 and SZ8 (Fig. 8a). *Xestoleberis hanaii* was abundant in outer-central bay stations, Shenzhen side, including SZ7, SZ8, and DB9 (Fig. 8b). *Propontocypris* sp. was relatively broadly distributed from inner to outer parts of the bay, with higher abundance observed in the outer region (Fig. 8c). *Pistocythereis*

240 *bradyformis* tended to show higher abundance in the ourter bay and at the bay mouth, while it was absent in most parts of the inner bay and at the Hong Kong side stations (Fig. 8d). *Spinileberis quadriaculeata* was abundant in central-outer bay stations SZ7 and SZ8 (Fig. 8e). *Hemicytheridea reticulata* was abundant in central bay stations SZ6, SZ7 and DB11 (Fig. 8f). *Loxoconcha sinensis* was distributed in the middle part of the bay, Shenzhen side, with high abundance observed in a relatively inner station SZ4 and one outer station SZ8 (Fig. 8g). *Loxoconcha ocellata* was abundant in outer bay stations SZ7

245 and SZ8 (Fig. 8h). *Aurila* cf. *disparata* was mostly found in station DB11 (Fig. 8i). Shenzhen side stations SZ7 and SZ8 had a distinct characteristics with relatively high abundance of *Stigmatocythere bona*, *Xestoleberis hanaii*, *Spinileberis quadriaculeata* and *Loxoconcha ocellata.* The bay mouth, particularly the oceanic-influenced stations DB14 and DB15, exhibited a distinctly high abundance of *Keijella kloempritensis* and *Pistocythere bradyi*. These stations also recorded highest total ostracod abundance.

250
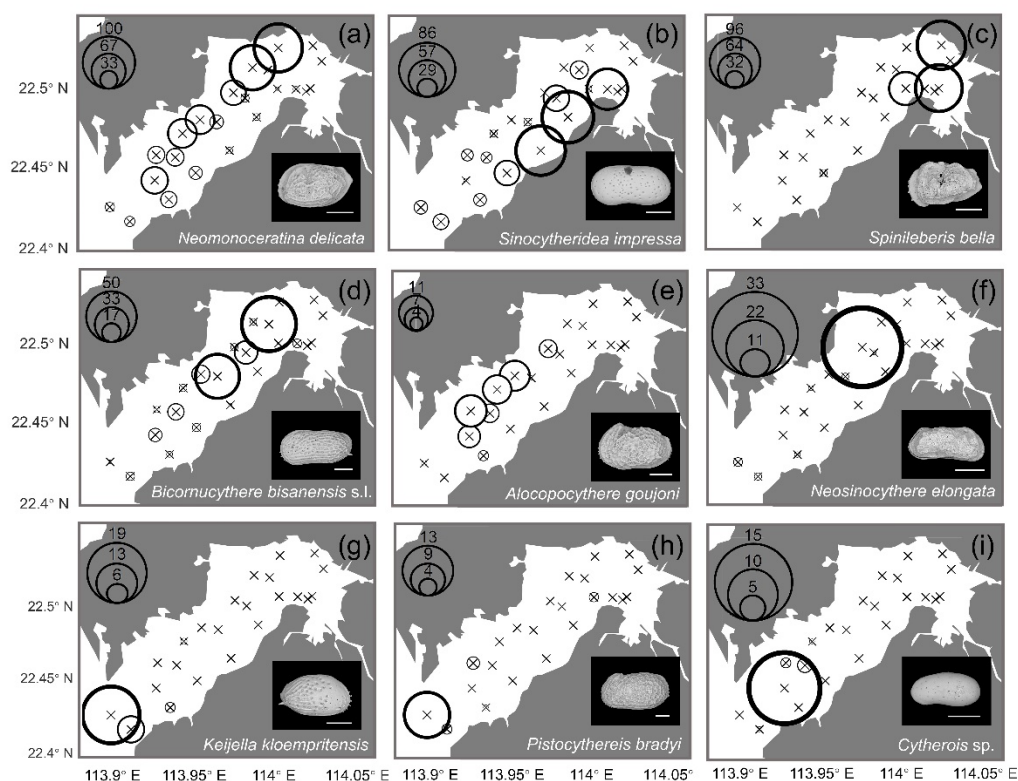
Figure 7. Spatial distribution of the relative (%) abundance for the top 9 abundant species (relative abundance over than 1% among all species) in Deep Bay. Including (a) *Neomonoceratina delicata*, **(b)** *Sinocytheridea impressa*, **(c)** *Spinileberis bella*, **(d)** *Bicornucythere bisanensis* **s.l., (e)** *Alocopocythere goujoni*, **(f)** *Neosinocythere elongata*, **(g)** *Keijella kloempritensis*, **(h)** *Pistocythereis bradyi*, **and (i)** *Cytherois* **sp.. The scale bar represents 200 μm for scanning electron microscope images at the lower-right corner of each subplot.**
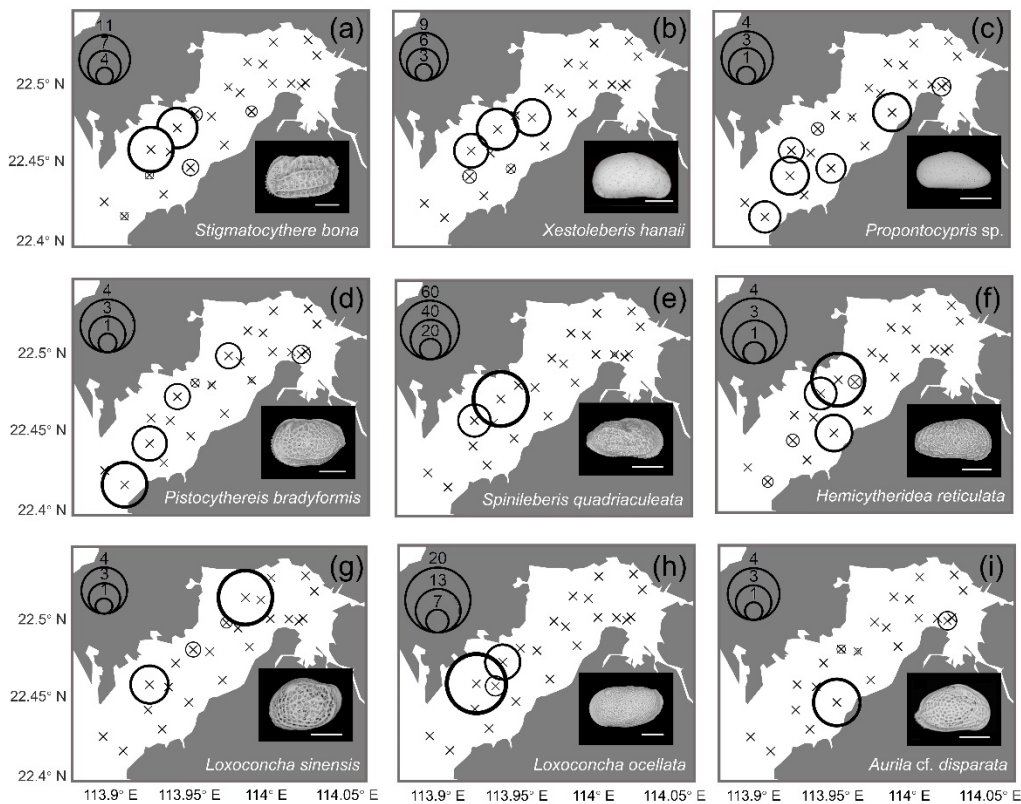
Figure 8. Spatial distribution of the relative (%) abundance for top 10–18 abundant species (relative abundance over than 0.3% among all species) in Deep Bay. Including (a) *Stigmatocythere bona,* **(b)** *Xestoleberis hanaii,* **(c)** *Propontocypris* **sp., (d)** *Pistocythereis bradyformis,* **(e)** *Spinileberis quadriaculeata,* **(f)** *Hemicytheridea reticulata,* **(g)** *Loxoconcha sinensis,* **(h)** *Loxoconcha ocellata,* **and (i)** *Aurila* **cf.** *disparata.* **The scale bar represents 200 μm for scanning electron microscope images at the lower-right corner of each subplot.**

4 Discussion

4.1 Abundance and diversity

Both ostracod abundance and diversity distribution followed a riverine-oceanic gradient in Deep Bay, driven by riverine input of excessive human waste leading to eutrophication and pollution (Note that the bay mouth area of Deep Bay is a part of Pearl River estuary but is still much more oceanic compared to the inner part of Deep Bay) (Figs. 4, 5). Recent studies showed that large amounts of nitrogen and phosphorus are transported to the inner-most part of Deep Bay by rainwater-runoff mainly via Shenzhen River from urban catchments, inducing eutrophication (Xu et al., 2019). Hypoxia frequency and

nutrient concentration were much higher in the inner-bay, river-influenced sites as shown in the 10 years averaged EPD data (Fig. 2a, b), indicating that eutrophication and hypoxia already became a long-term environmental problem in Deep Bay. In Asian urban marginal marine areas, eutrophication has been identified as one of the main drivers altering benthic ostracod

275 community, both contemporarily and historically (Yasuhara et al., 2007; Cheung et al., 2019; Hong et al., 2022). Ostracod abundance and diversity (Hill number ^{1}D and ^{2}D) of the entire bay had a significantly negative correlation with TOC content in sediments which also supported our perspective (Fig. 10). Metal pollution was investigated to be the dominant environmental factors structuring meiobenthic diversity in Hong Kong coastal waters (Hong et al., 2021; Hong et al., 2022). Relevant investigations in Deep Bay also showed a riverine-oceanic gradient on heavy metal pollutants and PFAs (Zhang et

280 al., 2021; Li et al., 2024), suggesting that the riverine-oceanic distribution of ostracod abundance and diversity may result from the combined effect of both eutrophication and pollution. We compared Hill Number values between riverine and oceanic sites (Figs. 9b, 11), we found that the diversity in oceanic sites was substantially higher when Hill Number order was low. The diversity between riverine and oceanic sites was almost the same in higher order Hill Numbers, indicating that eutrophication did not influence much of the structure of the dominant species among stations. This difference in diversity

285 between riverine and oceanic sites was mostly because of rare and abundant species. Low salinity and very shallow intertidal water depth could also be a reason for the lower diversity in riverine sites (Fig. 2c), as brackish-water environment is commonly characterized by much lower diversity compared to full-marine environment (Frenzel and Boomer, 2005; Whitfield et al., 2012) and aerial exposure at low tides could be stressful for marine organisms (Tomanek and Helmuth, 2002).

290
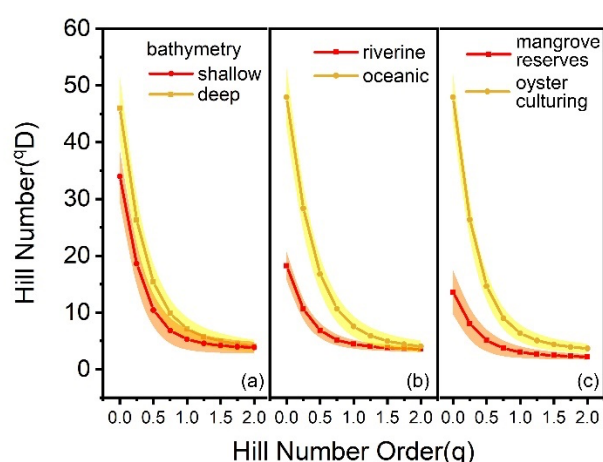
Figure 9. Hill number profile of deep-shallow bathymetry, riverine-oceanic area and mangrove reserves-oyster culturing zone. The shaded areas show 95% confidence interval of the profile. (a) Deep bathymetry indicates topography lower than PRL while shallow bathymetry indicates higher than PRL. (b) Riverine stations included stations inner than DB9 (DM3) while oceanic
295 **included stations outer and DB9 itself. (c) Stations in mangrove reserves included DB1–4 and SZ1–3 while other stations were regarded as oyster culturing zone.**
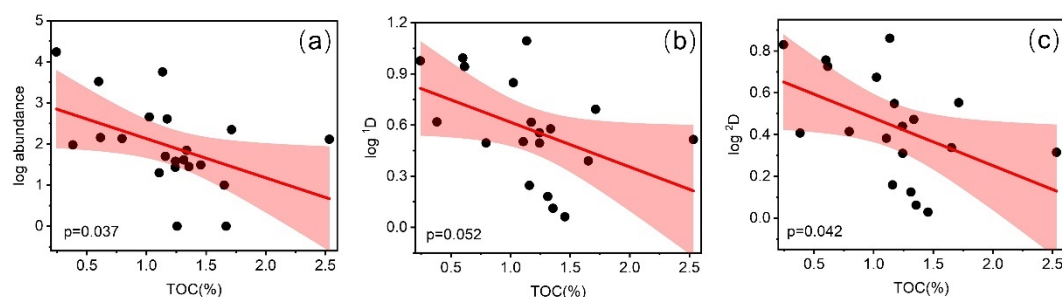
Figure 10. Relationship between eutrophication [total organic carbon (TOC) content in sediment] and abundance/diversities (Hill number ^{1}D and ^{2}D). (a) Total abundance vs. TOC. (b) Hill number ^{1}D vs. TOC. (c) Hill number ^{2}D vs. TOC. Shaded area shows 95% confidence interval.

4.2 Faunal distribution

In our study, three eutrophication/hypoxia tolerant species *Neomonoceratina delicata*, *Sinocytheridea impressa* and *Bicornucythere bisanensis* s.l. (Irizuki et al., 2003; Yasuhara et al., 2007; Yasuhara et al., 2012) were abundantly distributed in most of inner part of the bay where TOC was high (Figs. 3a, 7). The Sørensen dissimilarity result showed a distinction between riverine and oceanic (inner bay and middle-outer bay) stations (Fig. 6a). The outer-bay biofacies 5 in Sørensen dissimilarity was characterized by the lowest TOC and TN values, along with highest abundance and highest diversity. This biofacies exhibited oceanic characteristic and was less related to riverine eutrophication and pollution (Figs. 3a, c, 4, 5, 6a). In contrast, the inner-bay biofacies 3 in Sørensen dissimilarity was composed of brackish water species and related to almost all the eutrophication and pollution parameters that we used in this study, accompanied with high TOC and TN value, low abundance and low diversity (Figs. 3a, b, 4, 5, 6a, b). These results indicated that eutrophication and pollution were the drivers that differentiated the inner bay fauna from the outer bay ones. The inner-most bay biofacies 1 (of all dissimilarities) was probably a river month, brackish-water fauna, because it was located nearby Shenzhen River mouth and characterized by low salinity (Figs. 2, 6a, c, e). The dominant species in this biofacies was *Spinileberis bella* that is most likely a brackish-water species (Hou and Gou, 2007), as most *Spinileberis* species are known as brackish-water inhabitants (e.g., Zhao and Whatley 1988).

In addition to this major faunal trend of the inner-outer bay gradient, another major faunal trend was the separation of Hong Kong side and Shenzhen side faunas, clearly represented as biofacies 3 and 4, respectively, in the Horn and Morisita-Horn dissimilarity results (Fig. 6c, d). Correspondingly, Hong Kong side stations were more eutrophication-influenced while Shenzhen side stations were more affected by heavy metal pollution (Fig. 6d, f). Biofacies 3 showed the highest abundance

325   in eutrophication-tolerant *Sinocytheridea impressa* (Hong et al., 2019) in both Horn and Morisita-Horn based cluster analysis (Table 1), indicating that the Hong Kong side benthic ecosystem was influenced more by eutrophication. In contrast, biofacies 4 was characterized by a very high abundance in metal-pollution-tolerant *Neomonoceratina delicata* (Hong et al., 2019) and a much lower abundance of *Sinocytheridea impressa* (Table 1), indicating that the Shenzhen side benthic ecosystem was influenced more by metal pollution. Most eutrophication parameters were related to biofacies 3 in the Hong

330   Kong side, including hypoxia frequency, *Chla*, DIN, and related sediment eutrophication parameters including TC, TN and TOC (Fig. 6d, f). Pollutant PFAs and heavy metal Cu, Zn, Pb, Cr, As were related to biofacies 4 in the Shenzhen side (Fig. 6d, f), and TS was also related to biofacies 4, potentially because heavy metal availability affects sediment sulfur cycle (Jørgensen et al., 2019).

335   The reason for the distinction between the Hong Kong side and Shenzhen side remained unclear due to limited evidence. However, there are several possibilities. Stations in biofacies 3 (Hong Kong side) were shallower than staitons in biofacies 4 (Shenzhen side) (Zhang and Mao, 2015) (Also see Fig. 1). With shallower water depth in the Hong Kong side, organic matter could be less decomposed in the water column with its short distance from the surface water to the bottom sediment, resulted in higher sedimentation of organic materials in the sediments compared to the deeper Shenzhen side. It is also

340   shown in sedimentary TOC and TN result, with shallower Hong Kong side stations having relatively high TOC and TN concentrations compared to the Shenzhen side stations (Fig. 3a, c), indicating a more eutrophic condition in the Hong Kong side. Notably, α diversity was lower at shallower water depth (Figs. 9a, 11), potentially because of the stress from eutrophication. Another difference is that the Shenzhen side of Deep Bay is surrounded by Futian and Nanshan district, which are two of the most populated districts of Shenzhen City (Zhou et al., 2020). Comparably, Hong Kong side of Deep

345   Bay is close to Hong Kong rural area. Moreover, secondary industry was transferred from Hong Kong to Shenzhen after 1978 (Sit et al., 2020). Now secondary industry accounts for 37.6% GDP in Shenzhen which is almost 5 times higher than 6.5% in Hong Kong (data from the website of the Greater Bay Area https://www.bayarea.gov.hk/sc/home/index.html). More industrial waste could be the reason of pollutant-driven ostracod fauna distribution in Shenzhen side. Possible roles of oyster aquaculturing were uncertain, because oyster aquaculture rafts distribute almost cross the entire Deep Bay except at the

350   inner-most bay, mangrove area (Fig. 1). Although diversity was much higher in the oyster aquaculture sites compared to the inner-most bay mangrove sites (Figs. 9c, 11), it might be complicated by the fact that mangrove sites were characterized by low salinity, acidic condition, and intertidal water depth as discussed earlier.

4.3 Comparison with broader Hong Kong study

355   Species distribution of ostracod species has been investigated in the broader Hong Kong region (Hong et al., 2019). While *Alocopocythere goujoni* was common in Hong Kong's western water, albeit with low abundance (Hong et al., 2019), we found that this species was most abundant in the middle-outer part of Deep Bay (Fig. 7e) among Hong Kong's waters (Hong

et al., 2019). Hong et al. (2019) suggested that this species is a high salinity indicator. Our study partially supports this finding, as *Alocopocythere goujoni* were abundant in the middle-outer Deep Bay. However, other factors may also be at play,

360   considering that Deep Bay is not the area with highest salinity in Hong Kong (Fig. 2c; Hong et al., 2019). *Neosinocythere elongata* was favourable to high turbidity condition in Hong Kong broadly (Hong et al., 2019), and was indeed distinctly abundant in inner-bay biofacies 6 in Horn dissimilarity in Deep Bay (Table 1). *Neomonoceratina delicata* broadly distributed in all of Hong Kong waters (Hong et al., 2019), and it also broadly distributed with relatively high abundance in Deep Bay (Fig. 7a). *Sinocytheridea impressa* and *Bicornucythere bisanensis* s.l. were more abundant in semi-enclosed bay areas, such

365   as Tolo harbour and inner Port Shelter in Hong Kong (Hong et al., 2019). Consistently, we found that they were also abundant mostly in the inner Deep Bay (Fig. 7b, c). In contrast, *Keijella kloempritensis* and *Pistocythereis bradyi* were distributed more in open waters, such as the southern and eastern part of Hong Kong, as they preferred deep waters and high salinity environments, respectively (Hong et al., 2019). Consistently, they distributed mostly at the bay mouth of Deep Bay (Fig. 7g, h). *Xestoleberis hanaii* had a preference of more transparent water condition in Hong Kong (Hong et al., 2019) and,

370   in our Deep Bay study, were located more in the deeper and less eutrophic Shenzhen side (Fig. 8b). *Propontocypris* sp., which preferred lower productivity in Hong Kong (Hong et al., 2019), was distributed more in the outer part of Deep Bay (Fig. 8c). In summary, we found consistent spatial trends of species distribution between our Deep Bay study and the previous broader Hong Kong study of Hong et al (2019). Phytal species such as *Cytherois* sp., *Xestoleberis hanaii* and *Aurila* cf. *disparata* were mostly distributed in oyster aquaculture areas (Figs. 1, 7i, 8b, i), which may be related to phytal habitats

375   associated with oyster rafts. However, this is speculative, as oyster aquaculture covers almost entire area of Deep Bay and not just the inner bay and mangrove areas (Fig. 1).

The wide distribution of ostracod biofacies in Hong Kong is complex and cannot be explained straightforwardly by one or two environmental factors (Hong et al., 2022). This complexity likely arises from the region's multiple enbayments,

380   complicated coastline, numerous small and large islands, and varied environmental regimes influenced by multiple sources of pollutants, nutrients, freshwater, etc. However, our high-resolution study in much simpler, smaller system as an important part of Hong Kong, i.e., Deep Bay, clearly confirmed that the river-influenced eutrophication is a critical factor controlling marginal marine benthic community. While intermediate level of eutrophication may be beneficial to soft sediment benthos, the excess food supply caused by eutrophication, along with the consequent bottom deoxygenation, can lead to the

385   dominance of a few opportunistic species, finally resulting in low diversity, as observed in East Asia and globally (Yasuhara et al., 2007, 2012). Riverine metal pollution may amplify this benthic community change and contributed to form the gradient of opportunistic species under stress in the inner part of the bay to healthier fauna in the outer part of the bay in Deep Bay.

390
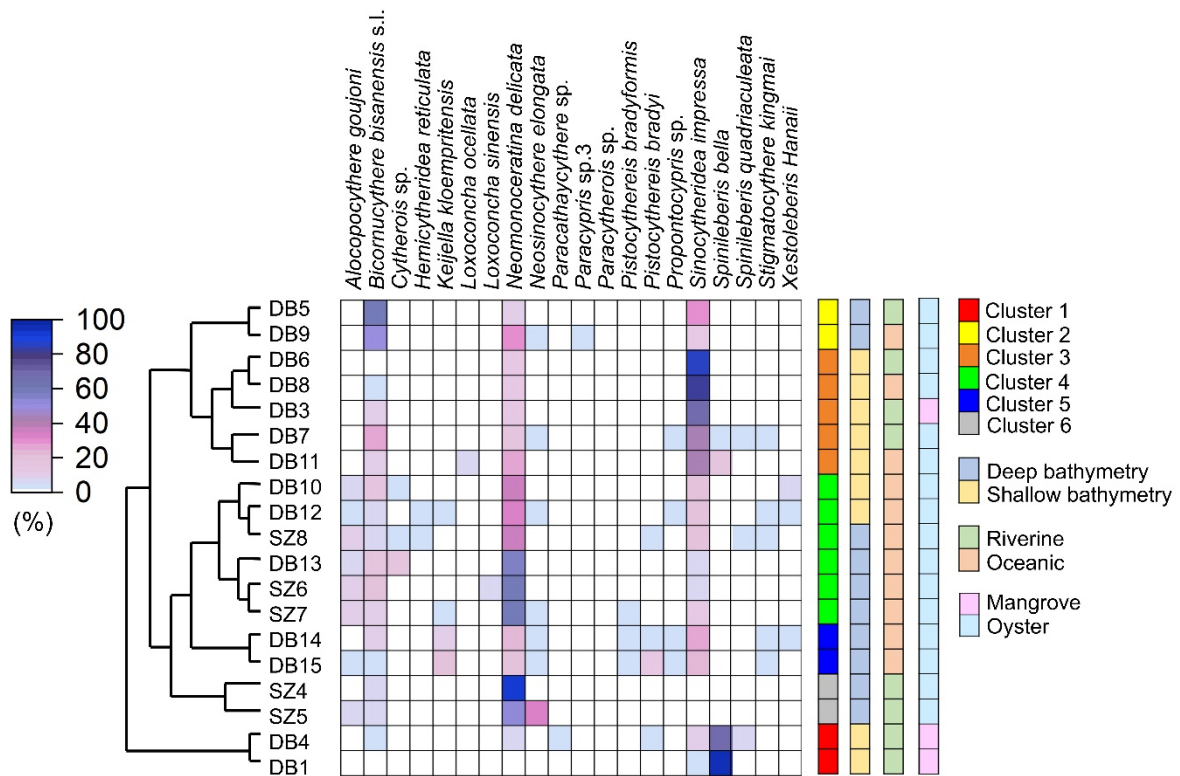
Figure 11. Heatmap with Horn dissimilarity among samples which shows top 10 species of highest mean relative abundance in each cluster. The side panel shows cluster details, bathymetry difference and riverine-oceanic circumstances of each sample.

5 Conclusion

395   Ostracod abundance, diversity, composition, distribution, as well as thier interactions with eutrophication and pollution, were investigated through high-resolution sampling of surface sediments in Deep Bay, a small semi-enclosed bay adjacent to two of the most populated cities in the world. We found that:

1.   Eutrophication and pollution were the most dominant drivers of ostracod abundance and diversity, creating a
400   pronounced inner-outer bay gradient in Deep Bay.

2. Faunal composition in Deep Bay was characterized by difference between the inner and outer bays, as well as between the Hong Kong and Shenzhen sides. The inner-outer difference was controlled by eutrophication along with pollution from rivers. The Hong Kong-Shenzhen side difference was associated with eutrophication in the Hong Kong side and metal pollution in the Shenzhen side. However, the mechanism and dominant factor driving the Hong Kong-Shenzhen gradient remained unclear.

3. Our results in Deep Bay were consistent with broader studies on ostracod diversity and distribuiton in Hong Kong, strongly supporting the idea that ostracod is an useful bioindicator of coastal benthic ecosystems. Moreover, in our smaller urban bay case, our investigation provided strong evidence of how eutrophication shapes benthic ostracod communities— an effect that may not be as apparent at larger spatial scales, especially in the regions with complicated geographic settings like Hong Kong, which features with multiple embayments, complex coast lines, and numerous islands. This underscores the importance of fine-scale sampling for regional studies. Eutrophication and pollution in small urban bay area have already caused profound consequences.

6 Acknowledgement

We thank Natalia Albarran-Melzer for help with sampling; Yuxuan Lin, Yafei Sun for help onboard; Rachel P. P. Wong, Lifang Wang, Zhe Wang, Qing Li for technical support. The work described in this paper was partially supported by Research Grants Council of the Hong Kong Special Administrative Region, China (project code: RFS2223-7S02), Seed Funding for Basic Research of the University of Hong Kong (project codes: 2302101483; 2202100581; 202111159167) and SKLMP Seed Collaborative Research Fund (project codes: SKLMP/SCRF/0073; SKLMP/SCRF/0055) (to MY) and funding from Research Grants Council of the Hong Kong Special Administrative Region, China (project code AoE/P-601/23-N) to MD.

References

Bowler, R. A., Yang, D. S. C., and Smith, A. J. E.: The pearl river estuary oyster industry in and around deep bay, Journal of the Hong Kong Branch of the Royal Asiatic Society, 162–181, http://www.jstor.org/stable/23902772, 1984.

Breitburg, D., Levin, L., Oschlies, A., Grégoire, M., Chavez, F., Conley, D., Garcon, V., Gilbert, D., Gutiérrez, D., Isensee, K., Jacinto, G., Limburg, K., Montes, I., Naqvi, S. W. A., Pitcher, G., Rabalais, N., Roman, M., Rose, K., Seibel, B., and Zhang, J.: Declining oxygen in the global ocean and coastal waters, Science (New York, N.Y.), 359, 10.1126/science.aam7240, 2018.

Chao, A., Gotelli, N., Hsieh, T. C., Sander, E., Ma, K., Colwell, R., and Ellison, A.: Rarefaction and extrapolation with Hill numbers: A framework for sampling and estimation in species diversity studies, Ecological Monographs, 84, 45–67, 10.1890/13–0133.1, 2014.

435 Chao, A., Kubota, Y., Zelený, D., Chiu, C. H., Li, C. F., Kusumoto, B., Yasuhara, M., Thorn, S., Wei, C.–L., Costello, M., and Colwell, R.: Quantifying sample completeness and comparing diversities among assemblages, Ecological Research, 35, 292–314, 10.1111/1440–1703.12102, 2020.

Cheung, R., Yasuhara, M., Iwatani, H., Wei, C.–L., and Dong, Y.: Benthic community history in the Changjiang (Yangtze River) mega–delta: Damming, urbanization, and environmental control, Paleobiology, 45, 1–15, 10.1017/pab.2019.21, 2019.

440 Cronin, T. and Vann, C.: The Sedimentary Record of Climatic and Anthropogenic Influence on the Patuxent Estuary and Chesapeake Bay Ecosystems, Estuaries and Coasts, 26, 196–209, 10.1007/BF02695962, 2003.

Dai, M., Zhao, Y., Chai, F., Chen, M., Chen, N., Chen, Y., Cheng, D., Gan, J., Guan, D., Hong, Y., Huang, J., Lee, Y., Leung, K., Lim, P. E., Lin, S., Lin, X., Liu, X., Liu, Z., Luo, Y.–W., and Zhang, Z.: Persistent eutrophication and hypoxia in the coastal ocean, Cambridge Prisms: Coastal Futures, 1, 1–71, 10.1017/cft.2023.7, 2023.

445 Dewiyanti, I., Darmawi, D., Muchlisin, Z., Zahrial, H., Imelda, I., and Defira, C.: Physical and chemical characteristics of soil in mangrove ecosystem based on differences habitat in Banda Aceh and Aceh Besar, IOP Conference Series: Earth and Environmental Science, 674, 012092, 10.1088/1755–1315/674/1/012092, 2021.

Dorgham, M: Effects of Eutrophication, in: Ansari, A. A. and Gill, S. (Eds.): Eutrophication: Causes, Consequences and Control, Springer Science & Business Media, USA, 29–44, 10.1007/978–94–007–7814–6, 2014.

450 Environmental Protection Department of Hong Kong: Marine Water Quality in Hong Kong 2024, available at: https://www.epd.gov.hk/epd/english/environmentinhk/water/hkwqrc/waterquality/marine.html, 2024.

Feng, Z., Tan, G., Xia, J., Shu, C., Chen, P., Wu, M., and Wu, X.: Dynamics of mangrove forests in Shenzhen Bay in response to natural and anthropogenic factors from 1988 to 2017, Journal of Hydrology, 591, 125271, 10.1016/j.jhydrol.2020.125271, 2020.

455 Frenzel, P. and Boomer, I.: The use of ostracods from marginal marine, brackish waters as bioindicators of modern and Quaternary environmental change, Palaeogeography, Palaeoclimatology, Palaeoecology, 225, 68– 92, 10.1016/j.palaeo.2004.02.051, 2005.

Frenzel, P., Keyser, D., and Viehberg, F.: An illustrated key and (palaeo)ecological primer for Postglacial to Recent Ostracoda (Crustacea) of the Baltic Sea, Boreas, 39, 567–575, 10.1111/j.1502–3885.2009.00135.x, 2010.

460 Glibert, P.: Eutrophication, harmful algae and biodiversity — Challenging paradigms in a world of complex nutrient changes, Marine Pollution Bulletin, 124, 10.1016/j.marpolbul.2017.04.027, 2017.

Hong, Y., Yasuhara, M., Iwatani, H., and Mamo, B.: Baseline for ostracod–based northwestern Pacific and Indo–Pacific shallow–marine paleoenvironmental reconstructions: ecological modeling of species distributions, Biogeosciences, 16, 585–604, 10.5194/bg–16–585–2019, 2019.

465   Hong, Y., Yasuhara, M., Iwatani, H., Chao, A., Harnik, P., and Wei, C.–L.: Ecosystem turnover in an urbanized subtropical seascape driven by climate and pollution, Anthropocene, 36, 100304, 10.1016/j.ancene.2021.100304, 2021.

Hong, Y., Yasuhara, M., Iwatani, H., Harnik, P., Chao, A., Cybulski, J., Liu, Y., Ruan, Y., Li, X., and Wei, C.–L.: Benthic ostracod diversity and biogeography in an urbanized seascape, Marine Micropaleontology, 174, 102067, 10.1016/j.marmicro.2021.102067, 2022.

470   Horn, H.: Measurement of "Overlap" in Comparative Ecological Studies, American Naturalist – AMER NATURALIST, 100, 10.1086/282436, 1966.

Hou, Y. and Gou, Y., 2007. Fossil Ostracoda of China. Volume 2: Cytheracea and Cytherellidae, Science Publishing House, Beijing, 1034 pp., ISBN 9787030191830, 2007

Irizuki, T., Nakamura, Y., Takayasu, K., and Sakai, S.: Faunal changes in Ostracoda (Crustacea) in Lake Nakaumi, 475   southwest Japan, over the last 40 years, Geoscience Report of Shimane University, 22, 149–160, 2003.

Irizuki, T., Ito, H., Sako, M., Yoshioka, K., Kawano, S., Nomura, R., and Tanaka, Y.: Anthropogenic impacts on meiobenthic Ostracoda (Crustacea) in the moderately polluted Kasado Bay, Seto Inland Sea, Japan, over the past 70 years, Marine Pollution Bulletin, 91, 10.1016/j.marpolbul.2014.12.013, 2014.

Jørgensen, B., Findlay, A., and Pellerin, A.: The Biogeochemical Sulfur Cycle of Marine Sediments, Frontiers in 480   Microbiology, 10, 849, 10.3389/fmicb.2019.00849, 2019.

Lee, S.: Carbon dynamics of Deep Bay, eastern Pearl River estuary, China. II: Trophic relationship based on carbon– and nitrogen–stable isotopes, Marine Ecology–progress Series – MAR ECOL–PROGR SER, 205, 1–10, 10.3354/meps205001, 2000.

Li, H., Wang, Z., Zhou, Y., Shi, C., Gan, H., Chen, F., Xing, L., Guo, D., Zhu, L., Wang, N., Fang, S., and Bao, R.: Spatial 485   distribution characteristics of perfluoroalkyl substances in bulk and grain size fractionated sediments in Shenzhen Bay, Marine pollution bulletin, 199, 115931, 10.1016/j.marpolbul.2023.115931, 2024.

Luo, L., Ke, C.–H., Guo, X., Shi, B., and Huang, M.: Metal Accumulation and Differentially Expressed Proteins in Gill of Oyster (Crassostrea hongkongensis) Exposed to Long–Term Heavy Metal–Contaminated Estuary, Fish & Shellfish Immunology, 38, 10.1016/j.fsi.2014.03.029, 2014.

490   Mamo, B., Cybulski, J., Hong, Y., Harnik, P., Chao, A., Tsujimoto, A., Wei, C.–L., Baker, D., and Yasuhara, M.: Modern biogeography of benthic foraminifera in an urbanized tropical marine ecosystem, Geological Society, London, Special Publications, 529, 10.1144/SP529–2022–175, 2023.

Mohyuddin, S., Mangi, A., Fahim, U., Khan, F., Rose, J., and Mao, Y.: Oyster bio–deposition enhanced the functional potential of labile and recalcitrant carbon in Shenzhen bay's sediments, Pakistan Journal of Science, 495   10.57041/pjs.v75i04.1031, 2023.

Morisita, M.: Measuring of dispersion of individuals and analysis of the distributional patterns, Mem. Fac. Sci. Kyushu Univ. Ser. E (Biol), 215–235, 1959.

Nichols, C., Zinnert, J., and Young, D.: Degradation of Coastal Ecosystems: Causes, Impacts and Mitigation Efforts, in, 119–136, 10.1007/978–3–319–75453–6_8, 2019.

500 Plazziat, J., Koeniguer, J., and Baltzer, F.: Des mangroves actuelles aux mangroves anciennes, Bulletin de la Societe Geologique de France, S7-XXV, 499-504, 10.2113/gssgfbull.S7-XXV.4.499, 1983.

Ren, H., Wu, X., Ning, T., Huang, G., Wang, J., Jian, S., and Lu, H.: Wetland changes and mangrove restoration planning in Shenzhen Bay, Southern China, Landscape and Ecological Engineering, 7, 241–250, 10.1007/s11355–010–0126–z, 2011.

Sit, V. F. S.: Industrial Transformation of Hong Kong, The Hong Kong–Guangdong Link, 163–186, 288pp.
505 ISBN9789622094017, 2020.

Sørensen, T. A.: Sørensen TJ. A method of establishing groups of equal amplitude in plant sociology based on similarity of species and its application to analyses of the vegetation on Danish commons. Biologiske Skrifter/Kongelige Danske Videnskabernes Selskab 5: 1–34, Kongelige Danske Videnskabernes Selskabs Biologiske Skrifter, 5, 1–34, 1948.

Tomanek, L. and Helmuth, B.: Physiological Ecology of Rocky Intertidal Organisms: A Synergy of Concepts, Integrative
510 and comparative biology, 42, 771-775, 10.1093/icb/42.4.771, 2002.

Wang, Q., Tsui, M., Ruan, Y., Lin, H., Zhao, Z., Ku, J., Sun, H., and Lam, P.: Occurrence and distribution of per– and polyfluoroalkyl substances (PFASs) in the seawater and sediment of the South China sea coastal region, Chemosphere, 231, 10.1016/j.chemosphere.2019.05.162, 2019.

Whitfield, A., Elliott, M., Basset, A., Blaber, S., and West, R. J.: Paradigms in estuarine ecology – A review of the Remane
515 diagram with a suggested revised model for estuaries, Estuarine, Coastal and Shelf Science, 97, 78–90, 10.1016/j.ecss.2011.11.026, 2012.

Xu, H., Zhang, Y., Zhu, X., and Zheng, M.: Effects of rainfall–runoff pollution on eutrophication in coastal zone: a case study in Shenzhen Bay, southern China, Hydrology Research, 50, 10.2166/nh.2019.012, 2019.

Yan, H., He, X., Lei, Y., Wang, Y., Su, H., and Jiang, S.: Land use–induced change in trophic state of Shenzhen Bay (South
520 China) over the past half–century, Marine Pollution Bulletin, 145, 208–213, 10.1016/j.marpolbul.2019.05.046, 2019.

Yang, Y., Gao, S., and Tong, X.: The Study on Hydrodynamic Characteristics of Qianhai Bay in Shenzhen, IOP Conference Series: Earth and Environmental Science, 768, 012011, 10.1088/1755–1315/768/1/012011, 2021.

Yasuhara, M., Hideo, Y., Tsujimoto, A., and Hirose, K.: The effect of long–term spatiotemporal variations in urbanization–induced eutrophication on a benthic ecosystem, Osaka Bay, Japan, Limnology and Oceanography, 52, 1633–1644,
525 10.4319/lo.2007.52.4.1633, 2007.

Yasuhara, M., Tittensor, D., Hillebrand, H., and Worm, B.: Combining marine macroecology and palaeoecology in understanding biodiversity: Microfossils as a model, Biological reviews of the Cambridge Philosophical Society, 92, 199–215, 10.1111/brv.12223, 2017.

Yasuhara, M., Hunt, G., Breitburg, D., Tsujimoto, A., and Katsuki, K.: Human–induced marine ecological degradation:
530 Micropaleontological perspectives, Ecology and evolution, 2, 3242–3268, 10.1002/ece3.425, 2012.

Ye, R., Zhang, C., Kong, J., Jin, G., Zhao, H., Song, Z.–y., and Li, L.: A non–negative and high–resolution finite volume method for the depth–integrated solute transport equation using an unstructured triangular mesh, Environmental Fluid Mechanics, 18, 10.1007/s10652–018–9598–4, 2018.

Zan, Q. J., Wang, B. S., Wang, Y. J., and Li, M. G.: Ecological assessment on the introduced Sonneratia caseolaris and S.
535 apetala at the Mangrove Forest of Shenzhen Bay, China, Acta Botanica Sinica, 45, 544–551, 2003.

Zhang, Q., Ren, F., Xiong, X., Gao, H., Wang, Y., Sun, W., Peifang, L., Li, Z., and Bai, Y.: Spatial distribution and contamination assessment of heavy metal pollution of sediments in coastal reclamation areas: a case study in Shenzhen Bay, China, Environmental Sciences Europe, 33, 10.1186/s12302–021–00532–9, 2021.

Zhang, S. and Mao, X.–Z.: Hydrology, sediment circulation and long–term morphological changes in highly urbanized
540 Shenzhen River estuary, China: A combined field experimental and modeling approach, Journal of Hydrology, 529, 10.1016/j.jhydrol.2015.08.027, 2015.

Zhao, Q. and Wang, P.: Distribution of Modern Ostracoda in the Shelf Seas off China, Developments in Palaeontology and Stratigraphy, 11, 805–821, 10.1016/S0920–5446(08)70223–1, 1988.

Zhou, Q., Xu, Y., Zheng, Y., Shao, J., Lin, Y., and Wang, H.: An Improved Method of Determining Human Population
545 Distribution Based on Luojia 1–01 Nighttime Light Imagery and Road Network Data–A Case Study of the City of Shenzhen, Sensors (Basel, Switzerland), 20, 10.3390/s20185032, 2020.